64;46

UCRL-JC-117034
PREPRINT

4504O 87175

Design and Modeling of Ignition Targets for the National Ignition Facility

S. W. Haan
S. M. Pollaine
J. D. Lindl
L. J. Suter
R L. Berger
L. V. Powers
W. E . Alley
P. A. Amendt
J. A. Futterman
W. K. Levedahl
M. D. Rosen
D. P. Rowley
R. A. Sacks
A. I. Shestakov
G. L. Strobel
M. Tabak
S. V. Weber
G. B. Zimmerman
W. J. Krauser
D. C. Wilson
S. Coggeshall
D. B. Harris
N. M. Hoffman
B. H. Wilde

This paper was prepared for submittal to
Physics of Plasmas

October 1994

Design and Modeling of Ignition Targets for the National Ignition Facility*

Steven W. Haan, Stephen M. Pollaine, John D. Lindl, Laurance J. Suter, Richard L. Berger, Linda V. Powers, W. Edward Alley, Peter A. Amendt, John A. Futterman, W. Kirk Levedahl, Mordecai D. Rosen, Dana P. Rowley, Richard A. Sacks, Aleksei I. Shestakov, George L. Strobel,* Max Tabak, Stephen V. Weber, George B. Zimmerman.
Lawrence Livermore National Laboratory, Livermore, CA 94550

William J. Krauser, Douglas C. Wilson, Stephen Coggeshall, David B. Harris, Nelson M. Hoffman, Bernhard H. Wilde
Los Alamos National Laboratory, Los Alamos, NM 87545

**Permanent address:*
University of Georgia, Athens, GA 30602

We have designed several targets that give yields of 1-30 MJ when indirectly driven by 0.9-2 MJ of 0.3 μm laser light. We describe the targets, the modeling that was used to design them, and the modeling we have done to set specifications for the laser system in the proposed National Ignition Facility. Capsules with beryllium or CH ablators are enclosed in gold hohlraums. All of our designs utilize a cryogenic fuel layer; we explain why it is very difficult to achieve ignition at this scale with a noncryogenic capsule. It is necessary to use multiple bands of illumination in the hohlraum to achieve sufficiently uniform x-ray irradiation, and to use a low-Z gas fill in the hohlraum to reduce filling of the hohlraum with gold plasma. Critical issues are hohlraum design and optimization, Rayleigh Taylor instability modeling, and laser-plasma interactions.

1. Introduction

The goal of the inertial confinement fusion (ICF) program is production of useful thermonuclear burn from a target driven with a laser or ion beam.[1,2] As a next step towards that goal, the ICF program has proposed a laser capable of producing ignition and intermediate gain.[3] The facility is called the National Ignition Facility (NIF). This article describes the ignition targets we have designed for the NIF, and the modeling we have done on them. We summarize the basic physics issues, and the following articles describe how these issues are being addressed with the Nova experimental program.[4,5] The baseline NIF target design is indirect drive, in which the laser light is used to heat a high atomic number enclosure called a hohlraum. A capsule in the hohlraum is imploded via ablation driven by the x-rays filling the hohlraum. The facility is being designed so that there also remains an option of doing direct drive ignition targets, with the laser light directly incident on a spherical capsule ablator. The direct drive targets are being designed at the University of Rochester.[6] This article describes only indirect drive designs.

The NIF, as currently proposed, is a 192 beam frequency tripled ($\lambda = 0.35$ microns) Nd:glass laser system specified so that its routine on-target energy and power is 1.8 MJ and 500 TW, appropriately pulse-shaped.[3] A scientific prototype of one of the NIF beams, the "Beamlet," is presently operational and will confirm and refine the NIF laser design before construction is initiated.[7]

The targets described here are all similar to the baseline target, shown in Fig. 1. (All of the relevant physics is described in more detail in Ref. 8.) A spherical cryogenic capsule, with DT gas, DT solid fuel, and an ablator, is in a cylindrical gold hohlraum with two laser entrance holes (LEH). The hohlraum peak radiation temperature (T_R) is 250-300 eV, with a shaped prepulse as needed for a low-entropy implosion. The ablation pressure brings the fuel shell to a velocity of $3\text{-}4\times10^7$ cm/s. The central part of the DT is then compressed and heated, forming a hot-spot which reaches ignition conditions of column density $\rho r \sim 0.3$ g/cm^2 and ion temperature ~10 keV. Then α deposition "bootstraps" the central temperature to more than 30 keV. The hot-spot density at ignition is typically 75- 100 g/cm^3. The hot-spot is tamped by a much colder main-fuel layer, with $\rho\Delta r \sim 1$ g/cm^2 and density ~1000 g/cm^3. The burn propagates into the main-fuel layer and 10-15% of the total DT mass is burned. The target shown in Fig. 1 produces 10-15 MJ of yield, depending on the modeling used to simulate it.

Ignition may be defined as a temperature increase of about a factor of two beyond the temperature that would be achieved without α-particle deposition. If yields of more than ~2 MJ are observed there will be no question of whether ignition has been achieved. At lower yields ignition could be verified by a series

of experiments varying a drive parameter (e.g. peak power) through an ignition threshold. Ignition would appear as an increase in yield, and in burn temperature as diagnosed via neutron time-of-flight spreading, as the ignition threshold was crossed. Ignition by this definition corresponds to yields of more than approximately 1 MJ, because these rapidly imploding systems reach nearly 10 keV even without α deposition.

Assuming the laser meets other specifications, the two most important laser parameters determining the margin for ignition are the total energy and the peak power.[8] Ignition requires both energy and power, as indicated in Fig. 2. The ignition region is bounded on one side by hydrodynamic instabilities: at low power the targets must have high in-flight aspect ratios (radius divided by in-flight shell thickness). The most important hydrodynamic instability is the Rayleigh-Taylor (RT) instability, since the high density shell is being accelerated by low density ablated material and then decelerated by the relatively low density hot-spot. Our RT modeling is described in more detail below. Ultimately, this boundary of the ignition region is determined by the capsule surface smoothness; Fig. 2 assumes the surface finish currently achieved on Nova capsules. On the other side, the ignition region is bounded by laser-plasma instabilities. Laser intensity and other parameters determining the instabilities (especially the electron density) depend primarily on the desired peak hohlraum T_R. Estimates of the laser-plasma instabilities, described below, indicates that laser-plasma instabilities will be acceptable in targets driven to at least 320 eV. This is the upper boundary of the ignition region in Fig. 2.

The smallest possible ignition target, at 0.8 MJ and 300 TW, would have no remaining margin for uncertainties or errors in the target modeling. We have specified the NIF at 1.8 MJ and 500 TW in order to provide margin for such uncertainties. As we will describe further below, this margin is adequate to cover our estimates of energetically significant uncertainties.

Because of length limitations, this article cannot possibly describe in depth all of the modeling we have done. This article summarizes our techniques and results. Detailed reports are being prepared on various aspects of the modeling, and a few results, as referred to below, have been published. In Section 2 we describe the targets in more detail. Sections 3-5 describe the design and modeling issues for the hohlraum, laser plasma instabilities, and hydrodynamic instabilities respectively. Section 6 is a conclusion.

2. Description of ignition targets

The baseline design, referred to as the PT ("Point-design target") in the following, is shown in Fig. 1. Cryogenic hardware, not shown, is external to the hohlraum. The spherical capsule is a doped CH ablator around a shell of solid cryogenic DT. The solid DT layer is self-smoothing, because of the β-smoothing effect.[9] The density of the central DT gas is controlled via the cryogenic

temperature. The hohlraum is filled with a 50-50 (atomic) mixture of helium and hydrogen. This gas conducts away the β decay energy before the laser pulse, and maintains the open hohlraum cavity during the implosion. The mixture of gases minimizes stimulated Brillouin scattering (SBS) as discussed below.

The PT uses 1.35 MJ of 3ω light. This is intermediate between the full 1.8 MJ and the "ignition cliff" at 800 kJ. We have concentrated most of our modeling on this intermediate scale target. It is sufficiently robust that we can make a good case for its ignition, while it leaves margin for uncertainty with a 1.8 MJ facility. Also, by using a relatively small target to set specifications for power balance, pointing, target fabrication quality, and so forth, we can be sure that these are set adequately.

An optimal radiation temperature profile for the capsule, used as input to our capsule modeling, and an input laser profile, are shown in Fig. 3. The target can tolerate moderate deviations from the nominal profile. For example, Fig. 4 shows the yield from integrated calculations (described in more detail in the following section) as the duration of the peak power portion of the pulse is varied.

The light coming in each LEH is in two cones, as shown in Fig. 1, and we can minimize time-dependent asymmetry in the x-radiation incident on the capsule by dynamically varying the relative brightness of the cones. About one third of the energy must go into the waist cones. The 192 beams are clustered in groups of four, so that there are effectively 8 spots in each of the inner cones, and 16 in the outer cones. We may use slightly separate wavelengths in the four beams in each spot to limit laser-plasma instabilities. The four beams combine at an angle corresponding to an effective f/8 optic.

Each beam is focused to an elliptical spot, which reduces the laser intensity without reducing the LEH clearance. The spot has a shape approximating a flat-top (probably a sixth order supergaussian), again to minimize the peak intensity while maximizing LEH clearance. The nominal spot is 500 μm by 1000 μm at best focus. Such a spot can be made with recently developed kinoform phase plate techniques.[10]

The pulse shape shown in Fig. 3 creates four shocks, with the final shock bringing the ablator up to peak pressure with sufficiently low DT entropy. The entropy requirement implies a corresponding requirement on the precision of the pulse-shaping. For optimal performance the shocks must be timed within about 200 ps. Adequate shock timing may not be predictable *a-priori* given uncertainties in opacity and equation of state, but is achievable with an experimental program using techniques currently in use on Nova.[11]

The CH ablator contains 0.25% bromine dopant. (Some Nova targets currently use bromine-doped CH.[12]) The dopant is used to control the stability of the ablator/DT interface. It reduces the preheat in the CH, and eliminates an

unstable density step at the CH/DT interface. The CH is assumed to contain 5% oxygen as an incidental fabrication by-product.

Modeling of a wide variety of other targets has been done at various levels of detail. Several important aspects of the target can be varied, giving different trade-offs of the remaining uncertainties in our understanding.

The size of the target, and the energy it uses, is a very important variable. Direct geometric scales of the PT produce good burn at any laser energy above about 700 kJ, as shown in Fig. 5. Various other target designs, as described in the following, are at various scales in the ignition range.

Beryllium generally performs somewhat better than CH as an ablator. (The point design uses a CH ablator because of fabrication experience with Nova.[13]) Be must be doped more heavily than CH, and radially varying the doping allows for complete optimization. Designs exist in which the Be is doped with Cu, which appears attractive from a fabrication point of view, and others with a mixture of Na and Br. In the most highly optimized targets, the additional performance margin obtained by using Be instead of CH is equivalent to about 25 eV in peak hohlraum T_R. The advantage is somewhat more at 250 eV than at 300 eV.

We can vary the convergence ratio (defined as the initial outer radius of the ablator, divided by the ignition time hot-spot radius) by varying the initial central DT gas density. Since reducing the convergence ratio reduces the final ρr, it also reduces the yield. If the initial gas fill is increased so that ignition is marginal, i.e. the yield is reduced from 15 MJ nominal to about 1 MJ, the convergence ratio of the PT is reduced from 35 at nominal to 25 . We can reduce it further, to about 20 at marginal ignition, by using a Be ablator target at 300 eV peak drive. These low convergence targets require gas densities that would initially be in vapor equilibrium with liquid DT (as opposed to solid for the point design), and fielding them will require some modifications in the fabrication and fielding technology. The triple-point gas density,[14] 0.68 mg/cm^3, corresponds to a PT yield of 10 MJ at convergence ratio 30.

Various peak drive temperatures are possible; high temperatures stress laser plasma instabilities while minimizing hydrodynamic instabilities, while low temperatures provide the opposite trade-off. The baseline is 300 eV, a compromise between the two constraints. We have designed capsules driven at temperatures as high as 400 eV, which appear to be very robust as regards hydrodynamic instabilities. Using doped Be as an ablator, we have designed targets driven at 250 eV for which ignition is nearly as robust as with CH at 300 eV. Laser-plasma instabilities are estimated to be very benign in the 250 eV hohlraum.

There is also a wide variety of possible pulse shapes. The pulse shown in Fig. 3 has four peaks, each at a time and power to launch a shock as needed for the

low entropy implosion. Many other pulses can result in the same shocks in the fuel. We can use shorter pulses at higher powers (sometimes called "picket fence pulses"); we have used steps with the power held constant for a few ns in each step; at the other extreme, we have used pulses in which the power increases smoothly from an initial 10 TW up to peak power. Each of these shapes represents a different tradeoff of laser, hohlraum, and capsule physics.

We have also designed targets in which the solid DT fuel is supported in a foam layer.[15] This may be an important option if β layering is inadequate. DT-wettable foams of density 0.05 g/cm^3, with μm scale cell structure, have been fabricated and our designs assume this density. The foam targets work nearly as well as the solid DT targets. If β layering or some other technique can be used to maintain a pure DT layer about 10 μm thick, on the inside of a foam-supported main fuel layer, ignition occurs in clean DT and target performance is barely degraded at all by the presence of the foam. If all of the solid DT must be supported by foam, it is somewhat more difficult to ignite although targets at the PT scale still ignite with some remaining margin.

Finally, there are numerous possible ignition designs that have attractive features, and may actually perform better than the point design, but which are not as closely connected to the existing experimental data. Direct drive targets are an important option, pending experimental results from the Omega Upgrade at the University of Rochester. Other hohlraum designs are being investigated on Nova—for example, gold shields placed between the capsule and the LEHs can reduce the time-dependent asymmetry. Recent results on Nova for such a hohlraum are in excellent agreement with expectations based on simulations.[16] As the NIF is being planned and built, experiments on Nova will continue to refine our understanding of the target physics and will allow us to optimize the NIF design further.

So far we have described the various target options that work according to current modeling; we have also found two target concepts where our modeling predicts difficulties:

(i) We considered lining the hohlraum with CH, instead of the He/H gas fill described above. We find that the lining stagnates on axis, creating a pressure spike which perturbs the capsule implosion unacceptably. Unfilled hohlraums have too much Au absorption of the light. We intend to consider further both alternate liners and unfilled hohlraums with short, low temperature pulses.

(ii) In principle, it seems possible to achieve ignition with non-cryogenic gaseous DT. However, we have found that the implosion velocities required for ignition at the NIF scale result in high core temperatures before ignition ρr is reached, and then conduction out of the hot-spot is very high. In a cryogenic target, energy conducted out of the hot-spot into the DT pusher heats more DT—this increases the mass of the hot-spot, and the energy is not lost. If the hot-spot is

surrounded by inert material, the energy conducted out is not only lost from the fuel, but serves to degrade the compressibility of the pusher. RT instabilities would also be much more problematic if the igniting fuel were surrounded with inert material. Hence we have been unable to successfully calculate ignition in non-cryogenic capsules at the NIF scale.

We conclude this section with a brief description of our baseline 1D capsule simulations. These are done with the LASNEX code,[17] using Pn radiation transport,[18] equations of state calculated in-line with a "Quotidian EOS" package,[19] and average-atom XSN opacities.[20] We have also simulated the capsule implosion with other radiation transport schemes and see no difference from the Pn calculations. Implosion calculations use as a source non-Planckian frequency-dependent radiation determined from hohlraum simulations. The spectrum affects the short-wavelength hydrodynamic instability growth; other than this, the spectrum has little effect on target characteristics. We normally calculate the deposition of α particles produced by the burn with the multi-group diffusion package in LASNEX.[21] Hatchett[22] has run our baseline 1D simulation of the PT using a Monte-Carlo charged particle transport package,[23] and found that the ignition and burn is essentially the same as with multi-group charged particle diffusion.

Hohlraum design and modeling

The size of the hohlraum relative to the capsule is determined by a variety of tradeoffs. The required profile of radiation temperature vs. time is determined by the capsule, and any hohlraum larger than some minimum size could provide a given pulse shape. A larger hohlraum takes more laser energy and power, and the optimal size is a tradeoff of the energy and power requirements with the need for symmetry and acceptable plasma filling. Our modeling indicates that the symmetry and laser-plasma instabilities are acceptable in the baseline hohlraum. Assuming a 1.8 MJ, 500 TW NIF , there will be margin to increase the hohlraum size with the PT capsule, increasing the margin for laser-plasma instabilities or asymmetry. If necessary, we can further increase this margin by going to a smaller capsule, at the cost of either increasing hydrodynamic instabilities or developing Be-ablator fabrication technology.

Even with perfect laser pointing and beam-to-beam power balance, there is some asymmetry that we call the intrinsic asymmetry. This arises because of the LEH and the bright laser-irradiated spots (the LEH alone causes a 15% peak-to-valley asymmetry). As described in Ref. 8, the laser spots are placed to cancel the LEH asymmetry. The symmetry can be adjusted by changing the hohlraum length and the pointing of the beams. The quantities determining the intrinsic symmetry change in time: the LEH shrinks, the laser spots move due to plasma evolution, and the spots become less bright relative to the overall hohlraum brightness. With a single cone of beams, we found that the time-dependent

asymmetry was too large. Two cones of beams can be arranged to provide adequate symmetry. Also, with two cones the time-dependent asymmetry can be corrected dynamically by varying the relative power in the cones as a function of time. This detailed symmetry tuning will have to be done with a time-dependent symmetry campaign similar to those being done on the Nova laser.[4]

The best way to model the intrinsic asymmetry is with detailed two dimensional simulations with a radiation-hydrodynamics code such as LASNEX.[17] We use the best available radiation transport model for the hohlraum/capsule coupling, and simulations are continued all the way through burn. The simulations track the laser beams, calculating inverse Bremsstrahlung energy deposition and any refraction that occurs. We typically use XSN non LTE multi-group opacities,[20] although we have also done simulations with an opacity table derived from the STA opacity model.[24] Any coupling to the capsule via hydrodynamic pressure or electron conduction is included.

We have achieved adequate symmetry and good burn in such integrated simulations of a variety of designs: the PT at several scales as shown in Fig. 5, a Be design driven at 250 eV, another Be design at 300 eV, and a smooth-pulse 250 eV Be design. All except the PT scales shown in Fig. 5 use 1.1 to 1.5 MJ, at powers ranging from 365 to 500 TW. They give yields in the integrated simulations that are between 50% and 90% of clean 1D yields and show unambiguous ignition.

We must also model asymmetry resulting from imperfect power balance and pointing of the laser beams. In that case, we need to be concerned with fully three dimensional (3D) asymmetry. This asymmetry and its effects have been modeled in a variety of ways. The asymmetry can be estimated analytically, using laser spot brightnesses and positions determined from the 2-D LASNEX simulations. Also, the asymmetry can be calculated in 3D with a view-factor code.[25] We have used fully integrated calculations, as described above, to confirm the modeling and for some sensitivity studies. The actual asymmetry on the capsule is 3-D, and its effect on the implosion must be estimated with 2-D simulations of the implosion driven with an asymmetric radiation source.

We have imposed a wide variety of asymmetries on 2D capsule implosions, to ensure that the specified asymmetry levels are acceptable. We have seen a variety of ways in which asymmetry can affect the ignition. These include: the obvious kinematic effects of differing velocities; initiation of RT instability growth, especially evident during deceleration; mass flow toward less-driven regions, seeding RT instability; irregular hot-spot compression, sometimes forming jets that protrude from the core and disrupt the imploded configuration; and delayed ignition resulting in more RT growth. The maximum tolerable asymmetry depends on its temporal and spatial specifics; in brief summary, the capsule can tolerate less than about 1% time-averaged asymmetry, 5-10% time-dependent

swings in asymmetry that last for ~2 ns, and larger swings if they last much less than 2ns.

We do not find very much variation in sensitivity to asymmetry, among the various targets we have designed. Smaller capsules are slightly more sensitive to asymmetries that couple to deceleration RT growth. The difference is not large, and symmetry sensitivity is not an issue that is important in deciding the overall tradeoffs of laser size and power. Varying the hohlraum size, with a given capsule, is the symmetry issue likely to be more important in the tradeoffs.

Three-dimensional viewfactor calculations indicate that with nominal pointing errors each beam is to point within 50 μm of its nominal position, rms deviation—the resulting additional asymmetry on the capsule will be significantly less than 1%. This pointing specification also ensures more than adequate clearance of the LEH. This requirement is similar to that met by the Nova laser (30 μm rms,[27] which is 10 μrad, while 50 μm rms on NIF is 7 μrad because of the longer focal length).

Figure 6 shows an example of the 2D sensitivity determined from the integrated calculations, in this case for a Be-ablator target driven with a step laser power profile. The target can tolerate beam movement of several hundred microns, well outside the expected deviation given the pointing specification on the laser.

Three-dimensional viewfactor calculations also indicate that 10% rms power imbalance results in less than 1% asymmetry on the capsule, provided the deviations are uncorrelated among the 192 beams. The tolerable power imbalance can be much larger than this, depending on its temporal dependence. If there are correlations between the beams' powers, a much tighter power balance requirement is necessary. Groups of eight beams, with each group going into the same area of the hohlraum, must be balanced within about 3%. Generally the requirements are consistent with purely independent statistical deviations of the 192 beams; any correlations significantly beyond this may increase the asymmetry unacceptably.

These requirements on the laser are well within current Nova performance parameters of 3% rms energy imbalance, and 5-10% power imbalance over time scales that are generally less than half the pulse length.[27] This does not mean that symmetry in Nova'hohlraums is as good as in NIF hohlraums; the looser requirements for NIF are a result of the larger number of beams.

Asymmetries might also arise from laser-plasma interaction processes or other phenomena, such as RT instability at the Au/He interface, which are currently predicted not to be significant but for which uncertainty remains. Light can be scattered or it can be absorbed more or less efficiently at different positions in the hohlraum. The effect in all cases is equivalent to a power balance

change, a movement of the x-ray emission spots, or perhaps a spreading of the laser deposition spots (for small-angle side-scattering). Difficulties could arise only if these effects are so large that the irreproducible part of them is larger than the limits described above. If any of these processes occur but is reproducible and not too large, the effect can be compensated for by changing the hohlraum design parameters. Estimates based on Nova experiments and appropriate theory and modeling indicate that these processes can be kept within acceptable limits. If not, our ultimate recourse will be to increase the hohlraum size, reduce the laser intensity, and correspondingly reduce the hohlraum drive temperature.

Laser plasma instabilities

The most important laser-plasma scattering processes are stimulated Brillouin and Raman scattering (SBS and SRS) and filamentation. In SBS and SRS, the incident laser beam scatters from electron waves and ion waves respectively in the forward, side, or backscatter direction. Backscatter is calculated and observed to be the most unstable process, although sidescatter must be examined for its possible effect on capsule symmetry. SRS forward scatter is a very weak process; forward SBS is being evaluated for possible symmetry effects because of the exchange of energy between overlapping beams.[28] Filamentation or whole beam self focusing results from the refraction of the laser light into low density regions which are themselves produced by the pressure gradients from nonuniform laser heating or by ponderomotive forces. All of these processes are sensitive to the electron density and temperature, and laser intensity and wavelength.[29] In addition, SBS is sensitive to the electron-ion temperature ratio, velocity gradient, and the fraction of light and heavy ions in multiple species plasma.[30] In addition, we have shown with 3D filamentation simulations[31] that filamentation is sensitive to the speckle length (the axial length of a diffraction limited hotspot near the focal plane of the laser beam). The speckle length increases with the square of the f-number of the focusing system.

The laser must propagate through 3-5 mm of hot ($T_e \sim$ 3-5 keV at peak power), low density ($n_e \leq 1 \times 10^{21}$ cm^{-3}), low Z (mixture of helium and hydrogen) plasma. The density is about .05 critical over most of the beam path. For the inner ring of beams, the density gets as high as 15% of critical for the last millimeter of pathlength. However by this point the individual laser beam intensity has decreased substantially from its peak of 2×10^{15} W/cm^2.

The electron waves in these hot, low density plasmas are strongly damped. As a result the SRS gain is modest and comparable to gain that is routinely encountered in Nova experiments for which SRS backscatter levels are less than 1%. The hot electron fraction, which correlates well with the SRS light and integrates over all angles of scatter, is also less than 1% in these experiments.

SBS in these plasmas is not controlled by strong velocity gradients as it is in many exploding foil experiments[32] but by the strong ion acoustic wave damping provided by the hydrogen in the two species (HeH) plasma. To ensure adequate SBS levels, we fielded experiments with three different targets that had scalelengths, electron temperatures, electron densities, and gain exponents close to those calculated for the NIF point design.[33-35] The SBS and SRS were measured to be acceptably small (an order of magnitude smaller than tolerable). Peak SBS values were ~5% for C_5H_{12} gas targets (<2% time integrated); SRS reflectivities were even smaller. These experiments also demonstrated the influence of low Z gas mixtures[34]; targets filled with CO_2 had SBS reflectivities as high as 20%.[34,35] In the hohlraum experiments, the laser energy was observed to propagate to the gold wall in a time that agreed with LASNEX and to produce the expected spot size. Thus filamentation appears to be stable, in agreement with expectations based on our simulations.

Modeling of hydrodynamic instabilities

The shell is subject to RT instability on the outside during its acceleration, and on the inside during deceleration. There is also Rictmyer-Meshkov (RM) instability at all interfaces. (These instabilities are reviewed in Ref. 36.) Short wavelength RT growth in these capsules is stabilized by ablation of material through the unstable interface, and by the finite scale length on the ablation front. This stabilization has become quite well documented, both experimentally[37] and calculationally.[38] During deceleration, the growth of short wavelengths is also reduced from classical RT since the unstable interface is between two DT regions, the hot-spot and the main fuel, and again there is ablation (driven by electron conduction in this case) and a finite gradient scale length. Also, perturbations that grow on the outside must couple through the shell to affect the ignition, and short wavelength modes couple less effectively. These effects all reduce the impact of the short wavelengths, so that the system is only weakly nonlinear. The targets have been designed so that this is the case.

We have based our modeling on linear analysis that is as accurate as possible, with an extension into the weakly nonlinear regime as necessary. The linear analysis is based on a decomposition of the surface perturbations into spherical harmonics, which are eigenmodes of the linear evolution. We determine single mode growth by running many 2D simulations, each of one single mode in the linear regime throughout the simulation. This provides the most accurate calculation of all known effects, including stabilization, RM growth, and convergence effects. This set of calculations provides a spectrum of growth factors, which we combine with an assumed initial surface spectrum to determine the ignition time perturbation. Using a non-linear saturation model from Ref. 39, we determine whether the perturbations are nonlinear and estimate the nonlinear saturation. This results in a curve of ignition-time perturbation amplitude as a function of initial perturbation amplitude.

In order to test the weakly nonlinear analysis, we also run full simulations of multi-mode perturbations with realistic initial amplitudes. Currently simulations must be 2D, and the number of modes that can be included is limited. We have run a variety of multi-mode simulations on several capsules, at solid-angles ranging from relatively small conic sections to half-spheres. Results are consistent with the modeling described above, although further substantiation is an area of current work. Recent development of 3D codes will allow testing of possible differences between 2D and 3D evolution.[40]

We must also estimate how the perturbations around the hot-spot at ignition time will affect the ignition. The unstable interface is between relatively cold, dense DT and the hot, lower density DT of the hot-spot. Material mixing of different elements is not occurring, and there is only thermal mixing. The actual perturbations are three dimensional, and multi-mode, and the weakly nonlinear perturbation growth analysis indicates that the spectrum is strongly dominated by modes around l=10 to 15. The 3D character cannot be fully represented in any existing code; available 3D codes do not include all of the relevant physical processes. There is experimental[37] and calculational[40] evidence that the multi-mode 3D perturbation is probably an array of spikes penetrating in towards the hot-spot center, surrounding approximately hexagonal bubbles. We have modeled this in 2D in five ways: (i) We simulate a single bubble of appropriate solid angle surrounded by a curtain of spike falling along a reflecting boundary condition. The circular cone represents approximately a multi-faceted 3D cone, of similar size and gross shape. (ii) We also run perturbations with the opposite sign: a spike on axis surrounded by a circular bubble. (iii) We simulate perturbations on the waist that represent long circular ridges and curtains. (iv) We continue through burn time the multi-mode 2D simulations mentioned above. (v) We do 1D modeling in which the thermal mixing caused by the perturbation growth is represented as an enhanced thermal conductivity in the perturbed region.

All of these approaches give similar results as regards how large a spike can be tolerated before ignition is quenched: the spikes penetrating the hot-spot can be 10 to 15 μm in amplitude (for the PT), compared to a hot-spot radius of 30 μm. Combined with the modeling described above, this corresponds to a maximum tolerable initial ablator surface roughness of 50-80 nm rms. This is to be compared with 30 nm rms on current Nova capsules.

We have also considered the bubble penetration from the outside of the shell at peak velocity. We find that the surface finish requirements for shell integrity during acceleration and for ignition are similar. This equivalence depends weakly on the shape assumed for the spectrum of initial perturbations.

Because we have modeled the perturbation growth and its effects with a variety of different approaches, and get generally consistent results, we are fairly

confident that our modeling is accurate. The modeling relies on 2D code simulations of linear-regime perturbation growth, and so it is very important that these be tested thoroughly. The dominant uncertainties are the dependence on the spectrum of the drive x-rays, and on zoning, resulting in a net uncertainty in the outer surface finish specification that we believe to be about a factor of two. Finally, of course, it is very important to test the modeling experimentally. A major fraction of the Nova program is oriented towards verifying this modeling, with a variety of experiments measuring perturbation growth and its effects in both planar,[37] cylindrical,(new) and spherical[5,12,41] geometry. Results from these experiments have been consistent with the modeling, and our confidence in the modeling continues to increase.

The modeling described so far pertains to surface perturbations that are initially on the outside of the ablator. Of course, there will be perturbations on the other interfaces, as well as material inhomogeneity and other fabrication defects. Any of these can be modeled in a conceptually identical way, using LASNEX simulations that assume the existence of the perturbation of interest. We have determined that the capsule tolerates perturbations initially on the other interfaces which are much larger than tolerable perturbations initially on the outside. Perturbations on the DT/CH interface are very unlikely to be large enough to matter. Perturbations on the DT gas/solid interface need to be less than about 0.5 μm, which is somewhat smoother than current estimates of the smoothness of β layer surfaces.[42] Achieving a sufficiently smooth inner DT surface is therefore an outstanding target fabrication issue.

In summary, we see that the PT has a factor of about two margin in surface finish beyond surface finishes on the best current Nova capsules. The requirement on the DT gas/solid interface is much looser, with much less growth, but we have less control over the quality of this interface and it may actually be more difficult to meet the specification.

Conclusion

Given the experimental substantiation described in the following papers and other references above, we have good reason to expect ignition with a 1.8 MJ, 500 TW laser. Such a facility will provide an adequate safety margin above where modeling supported by those experiments indicates the ignition threshold to be, and this margin is sufficient to cover estimated uncertainties.

The remaining uncertainties can be compensated for with changes in the target design that will be made after further Nova experiments, or after the NIF experiments begin. Some possible changes in the target design or performance will be energetically significant. These include:

(i) A factor of two in hydrodynamic instability growth (equivalent to a factor of two in surface finish, or a factor of two in the acceptable size of the bang-time

perturbations) shifts the ignition cliff from 0.8 MJ to about 1.0 MJ. Improvements in surface finish could probably recover the original margin.

(ii) The combined uncertainties in x-ray conversion and hohlraum wall loss are less than about 20% in energy.

(iii) Stimulated Brillouin scattering should be less than about 10%, based on the experiments described above.

(iv) Achieving the correct power balance between the inner and outer cones of beams may require reducing the power in one or the other, so that it cannot run at its full power. This may result in a net energy loss of 10 to 15%.

(v) An error in hohlraum optimization that requires increasing the LEH radius 50% would require an increase in laser energy of 15% to regain the same hohlraum temperature.

(vi) Similarly, increasing the hohlraum area by 35% increases the required laser energy by 15%.

Several other uncertainties are energetically insignificant. For example, the equation of state and opacity of the CH ablator are sufficiently uncertain that we expect to adjust the details of the pulse shape phenomenologically, but this will not significantly affect the performance requirements from the laser, or the target performance.

These errors, in combined effect, are consistent with the factor of two margin provided by a 1.8 MJ, 500 TW laser. Based on all available data and detailed simulations, 1.8 MJ should be adequate for ignition.

There are some issues which we are addressing to substantiate this conclusion further and to progress with plans for the facility. The DT ice smoothness is currently not acceptable, and more detailed modeling of these perturbations is needed along with fabrication technology development. We still need to make a final decision regarding the optimal cone-to-cone energy ratio, and beam angles, which will be built into the target chamber and will be difficult to change once detailed facility design is in progress. We are doing more detailed modeling at the 700-900 kJ scale, to substantiate the basic argument that ignition is possible at this scale and hence that we have a factor of two margin. In order to maximize our understanding of the options available to us, we are continuing to pursue other designs—for example, hohlraums with shields between the capsule and the LEH. Finally, we are pursuing more detailed modeling of the PT in three areas: further sensitivity studies with integrated calculations; modeling that includes both long wavelength asymmetry and short-wavelength mix; and further modeling of the RT instability with large multi-mode simulations. These results, along with the ongoing experimental program on Nova, will either lead to increasing confidence in the performance of the PT or will indicate what changes need to be made in the design.

Acknowledgments

This work was performed under the auspices of the U. S. Department of Energy by the Lawrence Livermore National Laboratory under contract W-7405-ENG-48.

References

1. J. H. Nuckolls, L. Wood, A. Thiessen, and G. B. Zimmerman, Laser Compression of Matter to Super-High Densities: Thermonuclear (CTR) Applications, *Nature* **239**, 129 (1972).

2. J. D. Lindl, R. L. McCrory, E. M. Campbell, Progress Toward Ignition and Burn Propagation in Inertial Confinement Fusion, *Physics Today*, Sept. 1992.

3. J. T. Hunt, K. R. Manes, J. R. Murray, P. A. Renard, R. W. Sawicki, J. B. Trenholme, and W. Williams, Laser Design Basis for the National Ignition Facility, Lawrence Livermore National Laboratory, Livermore, CA, UCRL-JC-117399 (1994).

4. A. Hauer et al., following article.

5. M. Cable et al., second article following.

6. C. P. Verdon, private communication (1994).

7. B. M. Van Wonterghem, J. R. Murray, D. R. Speck, and J. H. Campbell, "Performance of the NIF Prototype Beamlet," LLNL Report UCRL-JC-115580, 1994 American Nuclear Society Meeting and 11th Topical Meeting on the Technology of Fusion Energy, New Orleans, LA, June 19-23, 1994; C. E. Barker, B. M. Van Wonterghem, D. R. Speck, B. W. Woods, D. F. Browning, S. C. Burkhart, W. C. Behrendt, J. R. Murray, and J. H. Campbell, and I. C. Smith, "Third Harmonic Performance of a Large Aperture, Multipass Nd-Glass Laser," LLNL Report UCRL-JC-118196, prepared for the ASSL Conference in Memphis, TN, Jan. 29-Feb. 1, 1995.

8. J. D. Lindl, Development of the Indirect Drive Approach to ICF and the Target Physics Basis for Ignition and Gain on the National Ignition Facility, Lawrence Livermore National Laboratory, Livermore, CA 94550, submitted to *Phys. Plasmas* (1994).

9. A. J. Martin, R. J. Simms, and R. B. Jacobs, *J. Vac. Sci. Technol.* A 6 (3), 1885 (1988).

10. S. N. Dixit, J. K. Lawson, K. R. Manes, H. T. Powell, and K. A. Nugent, "Kinoform Phase Plates for Focal Plane Irradiance Profile Control," *Opt. Lett.* **9**, 417-419 (1994).

11. R. L. Kauffman, L. J. Suter, C. B. Darrow, J. D. Kilkenny, H. N. Kornblum, D. S. Montgomery, D. W. Phillion, M. D. Rosen, and R. Theissen, R. J. Wallace, and F. Ze, "High Temperatures in Inertial Confinement Fusion Radiation Cavities Heated with 0.35 μm Light," *Phys. Rev. Lett.* **73**, 2320-2323 (1994).

12. C. J. Keane, R. C. Cook, T. R. Dittrich, B. A. Hammel, W. K. Levedahl, O. L. Landen, S. H. Langer, D. H. Munro, and A. A. Sciott, to appear in *Rev. Sci. Inst.*

13. A. K. Burnham, J. Z. Grens, E. M. Lilley, *J. Vac. Sci. Technol.* A **5** (6), 3417 (1987).

14. P. C. Souers, *Hydrogen Properties for Fusion Energy*, University of California Press, Berkeley, CA (1986).

15. R. A. Sacks and D. H. Darling, *Nuc. Fus.* **27**, 447 (1987).

16. P. A. Amendt, T. J. Murphy et al., to be published in *Phys. Rev. Lett.*

17. G. B. Zimmerman and W. L. Kruer, *Comm. Plasmas Phys . Cont. Thermonuclear Fusion* **2**, 51 (1975).

18. D. S. Kershaw, "Flux Limiting on Nature's Own Way," Lawrence Livermore National Laboratory, Livermore, CA, UCRL-78378 (1976).

19. R. M. More, K. H. Warren, D. A. Young, and G. B. Zimmerman, "A New Quotidian Equation of State (QEOS) for Hot Dense Matter," *Phys. Fluids* **31** (10), 3059 (1988).

20. W. A. Lokke and W. H. Grasberger, "XSNQ-U: A Non-LTE Emission and Absorption Coefficient Subroutine," Lawrence Livermore National Laboratory, Livermore, CA, UCRL-52276 (1977).

21. E. G. Corman, W. B. Loewe, G. E. Cooper and A. M. Winslow, *Nucl. Fusion* **15**, 377 (1975).

22. S. P. Hatchett, private communication (1993).

23. G. B. Zimmerman, "Recent Developments in Monte-Carlo Techniques," Lawrence Livermore National Laboratory, Livermore, CA, UCRL-105616 (1990).

24. A. Bar Shalom, J. Oreg, W. H. Goldstein, D. Shvarts, and A. Zigler, *Phys. Rev.* **A** 40, 3183 (1989).

25. R. C. Kirkpatrick and C. A. Wingate, private communication (1980); R. C. Kirkpatrick, J. E. Tabor, E. L. Lindman, A. J. Cooper, "Indirect Solar Loading of Waste Heat Radiators," Proc. Space 88, published by the American Society of Civil Engineers, S. W. Johnson and J. P. Wetzel, ed. (1988); D. S. Bailey (1981), D. H. Munro and G. B. Zimmerman (1993), private communication.

26. J. E. Murray, M. C. Rushford, C. S. Vann, R. L. Saunders, J. A. Caird, Precision Beam Pointing, ICF Quarterly Report, Lawrence Livermore National Laboratory, UCRL-LR-105821-94-1 (1993).

27. J. A. Caird, R. B. Ehrlich, O. L. Landen, C. W. Laumann, R. A. Lerche, J. L. Miller, T. L. Weiland, H. T. Powell, Precision Nova Power Balance, ICF Quarterly Report, Lawrence Livermore National Laboratory, UCRL-LR-105821-94-1 (1993).

28. K. Marsh, C. Joshi, and C. J. McKinstrie, BAPS November 7-11, 1994 Minneapolis.

29. W. L. Kruer, *The Physics of Laser Plasma Interactions* (Addison-Wesley, NY, 1998).

30. E. A. Williams, R. L. Berger, R. P. Drake, A. M. Rubenchik, B. S. Bauer, D. D. Meyerhofer, A. C. Gaeris, and T. W. Johnston, "The Frequency and Damping of Ion Acoustic Waves in CH and Two-Ion-Species Plasmas," to be published in *Physics of Plasmas*, 1995; S. C. Wilks, W. L. Kruer, J. Denavit, K. Estabrook, D. E. Hinkel, D. Kalantar, A. B. Langdon, B. Montgomery, J. Moody, and E. A. Williams, "Nonlinear Theory and Simulations of Stimulated Brillouin Backscatter in Two and Three Species Plasmas, UCRL-JC-117313, April 28, 1994, to be submitted to *Phys. Rev. Lett.*

31. R. L. Berger et al., *Phys Fluids B* **5**, 2243 (1993).

32. R. P. Drake, D. W. Phillion, K. Estabrook, R. E. Turner, R. L. Kauffman and E. M. Campbell, *Phys. Fluids B* **1**, 1089 (1989); P. E. Young, K. G. Estabrook, W. L. Kruer, E. A. Williams, P. J. Wegner, R. P. Drake, H. A. Baldis, and T. W. Johnston, *Phys. Fluids B* **2**, 1907 (1990); W. Seka, R. S. Craxton, R. E. Bahr, D. L. Brown, D. K. Bradley, P. A. Jaanimagi, B. Yaakobi, and R. Epstein, *Phys. Fluids B* 4, 432 (1992); H. A. Baldis, D. M. Willeneuve, B. La Fontaine, G. D. Enright, C. Labaune, S. Baton, P. Mounaix, D. Pesme, M. Cassanova, and W. Rozmus, *Phys. Fluids B* **5**, 3319 (1993).

33. L. V. Powers et al., "Low Stimulated Brillouin Backscatter Observed from Large, Hot Plasmas in Gas-Filled Hohlraums," submitted to *Phys. Rev. Lett.*

34. B. MacGowan et al., ECLIM 1994, Oxford, England.

35. J. Fernandez et al., ECLIM 1994, Oxford, England.

36. S. W. Haan, "Hydrodynamic Instabilities on ICF Capsules," Lecture Series on Inertial Fusion, Dept. of Astrophysical Sciences, Princeton University (1994).

37. B. A. Remington, S. V. Weber, S. W. Haan, J. D. Kilkenny, S. G. Glendinning, R. J. Wallace, W. H. Goldstein, B. G. Wilson, and J. K. Nash, *Phys. Fluids B* **5**, 2589 (1993).

38. S. V. Weber, B. A. Remington, S. W. Haan, B. G. Wilson, and J. K. Nash, "Modeling of Nova Indirect Dive Rayleigh-Taylor Experiments, to be published in *Phys. Plasmas* (1994); H. Takabe, K. Mima, L. Montierth, and R. L. Morse, "Self-Consistent Growth Rate of the Rayleigh-Taylor Instability in an Ablatively Accelerating Plasma," *Phys. Fluids* **28**, 3676 (1985); M. Tabak, D. H. Munro, and J. D. Lindl, "Hydrodynamic Stability and the Direct Drive Approach to Laser Fusion," *Phys. Fluids B* **2**, 5 (1990); J. H. Gardner, S. E. Bodner, and J. P. Dahlburg, "Numerical Simulation of Ablative Rayleigh-Taylor Instability," *Phys. Fluids B* **3**, 1070 (1991).

39. S. Haan, "The Onset of Non-Linear Saturation for Rayleigh-Taylor Growth in the Presence of a Full Spectrum of Modes, *Phys. Rev. A* **39**, 5812 (1989).

40. J. P. Dahlburg et al., this issue *Phys. Plasmas*; M. Marinak, private communication (1994).

41. T. R. Dittrich, B. A. Hammel, C. J. Keane, R. McEachern, R. E. Turner, S. W. Haan, L. J. Suter, "Diagnosis of Pusher-Fuel Mix in Indirectly Driven Nova Implosions, " *Phys. Rev. Lett.* **73**, 2324-2327 (1994).

42. G. W. Collins, E. R. Mapoles, J. Hoffer, J. Simpson, J. Sanchez, R. Bell, W. Unites, "Solid Hydrogen Surfaces," ICF Quarterly Report, Lawrence Livermore National Laboratory, UCRL-LR-105821-93-2 (1993).

Figure captions

1. An ignition target that uses 1.35 MJ of laser energy. The DT fuel is in a cryogenic layer, surrounded by a CH ablator doped with 0.25% Br. The capsule is suspended in the center of a gold hohlraum, which the incoming laser beams heat to 300 eV. The beams are arranged in two cones coming in from each side. This target is referred to as the PT in this article.

2. Total laser energy and peak power determine the margin for ignition. The region in which ignition can be achieved, according to current modeling, is indicated. Powers and energies along the indicated curve will be accessible to the NIF as currently planned. The dots indicate the laser's nominal operating point (1.8 MJ, 500 TW), and the energy and power assumed to be absorbed in the PT hohlraum.

3. Temperature vs. time optimal for the PT capsule, and laser power vs. time to drive the target. The shaped pulse prior to peak drive is needed to compress the target, increasing the pressure in a controlled way before applying peak power. The dashed curve is used as input to all capsule simulations, and the solid curve to hohlraum simulations.

4. Yield vs. duration of the peak power pulse, from integrated 2D simulations. the pulse width was changed by varying the cutoff time. The energy in a sample of the pulses is indicated. The failure at short pulse appears to be due to asymmetry, not energetic failure to ignite. Two different hohlraum lengths, providing different symmetry "tunes," are indicated.

5. Yield and burn-weighted ion temperature for geometric scales of the PT. The lines show 1D calculations of the capsule alone, in which linear dimensions and times are scaled together. Linear dimensions and times are scaled together. For these the horizontal scale is effective energy, that is, 1.35 MJ times the scale factor cubed. The dots are integrated calculations, plotted against the laser energy put into the simulation. For these linear dimensions and times were scaled, and laser powers were scaled as the square of the scale factor. Hohlraum length and cone-to-cone power ratios were adjusted to recover symmetry.

6. Yield in integrated simulations vs. pointing shifts, as indicated. At the indicated point the hohlraum length was changed to accommodate the shifted beams. The other points are in a fixed hohlraum. The midpoint between the two spots was kept fixed in these variations as were the laser powers and other dimensions. These calculations were done on a 300 eV beryllium-ablator target.

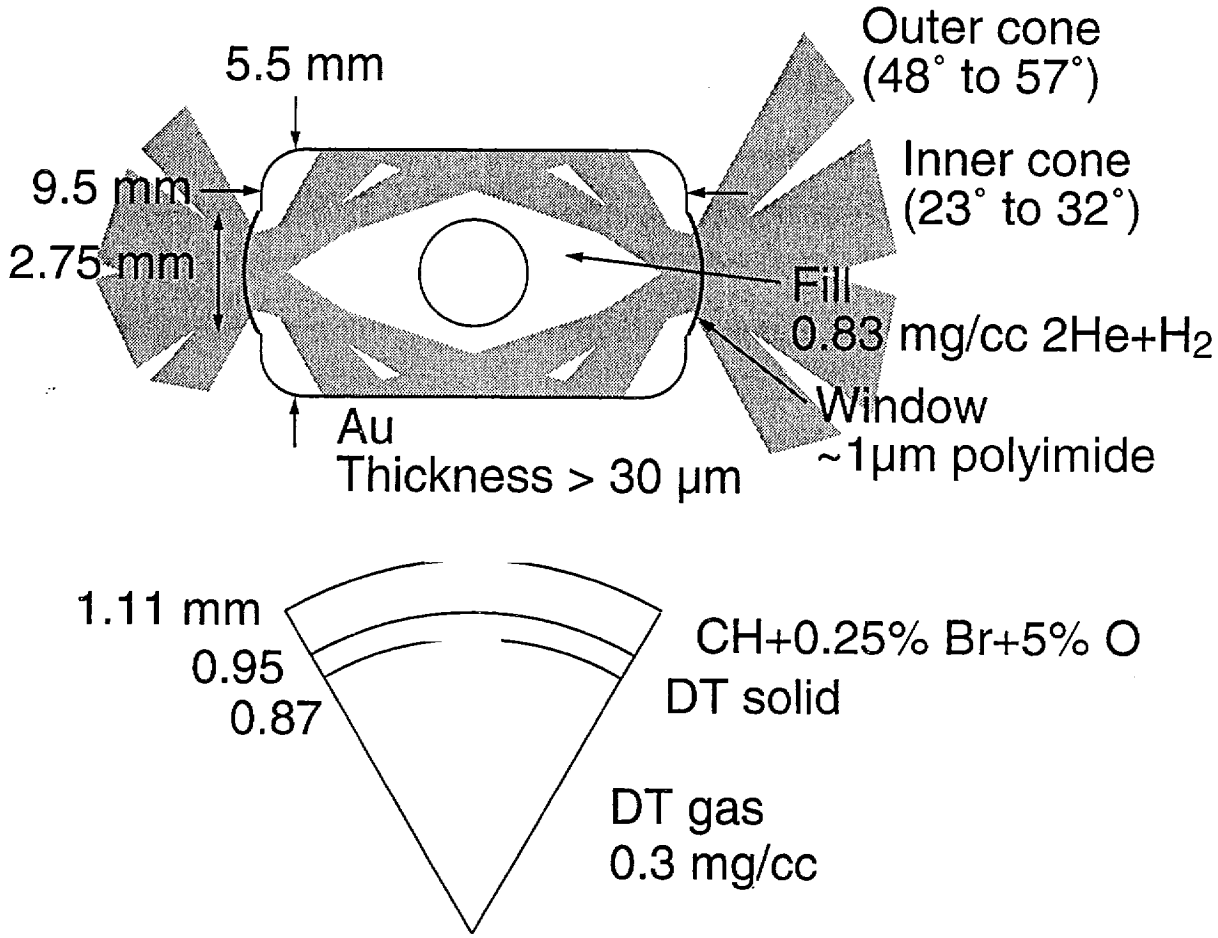
5.5 mm
Outer cone
(48° to 57°)
9.5 mm
2.75 mm
Inner cone
(23° to 32°)
Fill
0.83 mg/cc 2He+H2
Window
~1μm polyimide
Au
Thickness > 30 μm
1.11 mm
0.95
0.87
CH+0.25% Br+5% O
DT solid
DT gas
0.3 mg/cc

Fig. 1

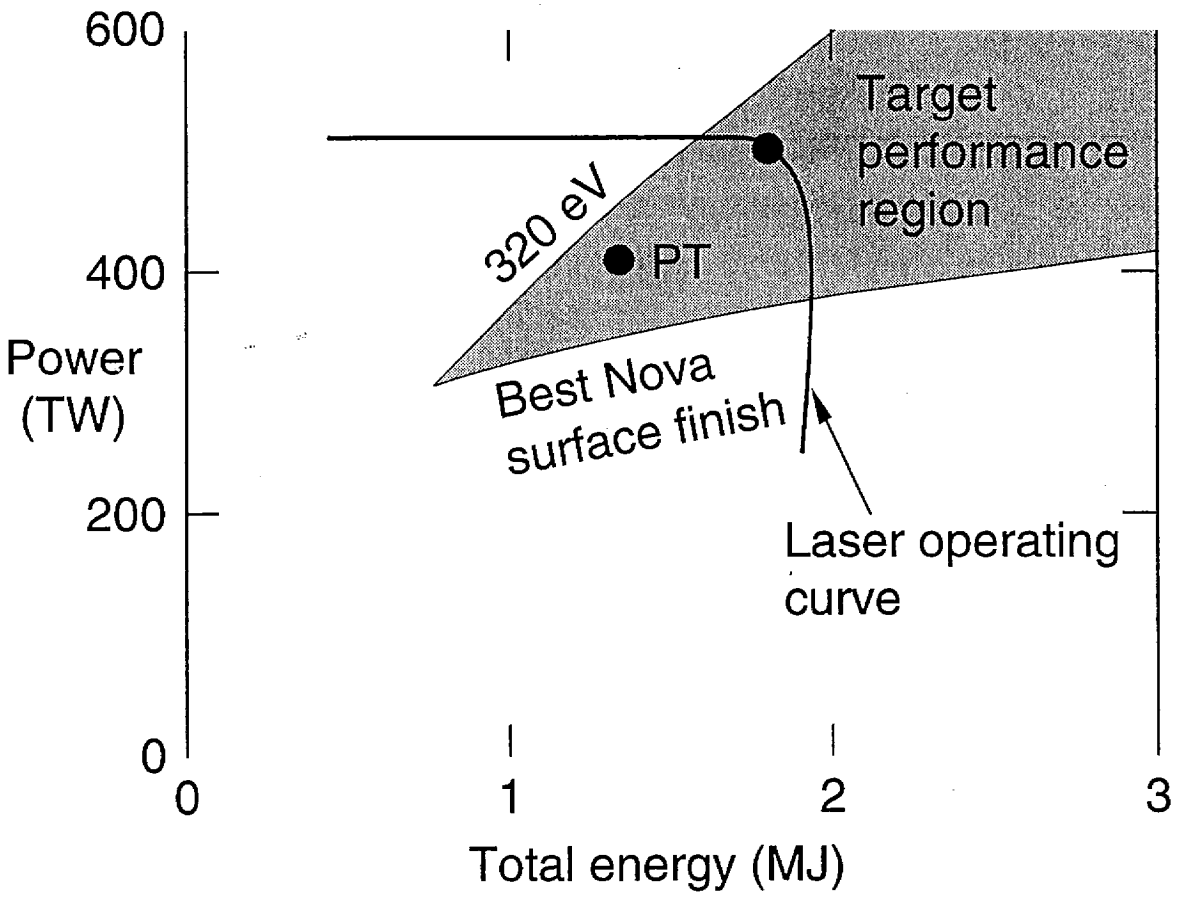
600
400
200
0
Power
(TW)
0
1
2
3
Total energy (MJ)
Target
performance
region
320 eV
PT
Best Nova
surface finish
Laser operating
curve

Fig. 2

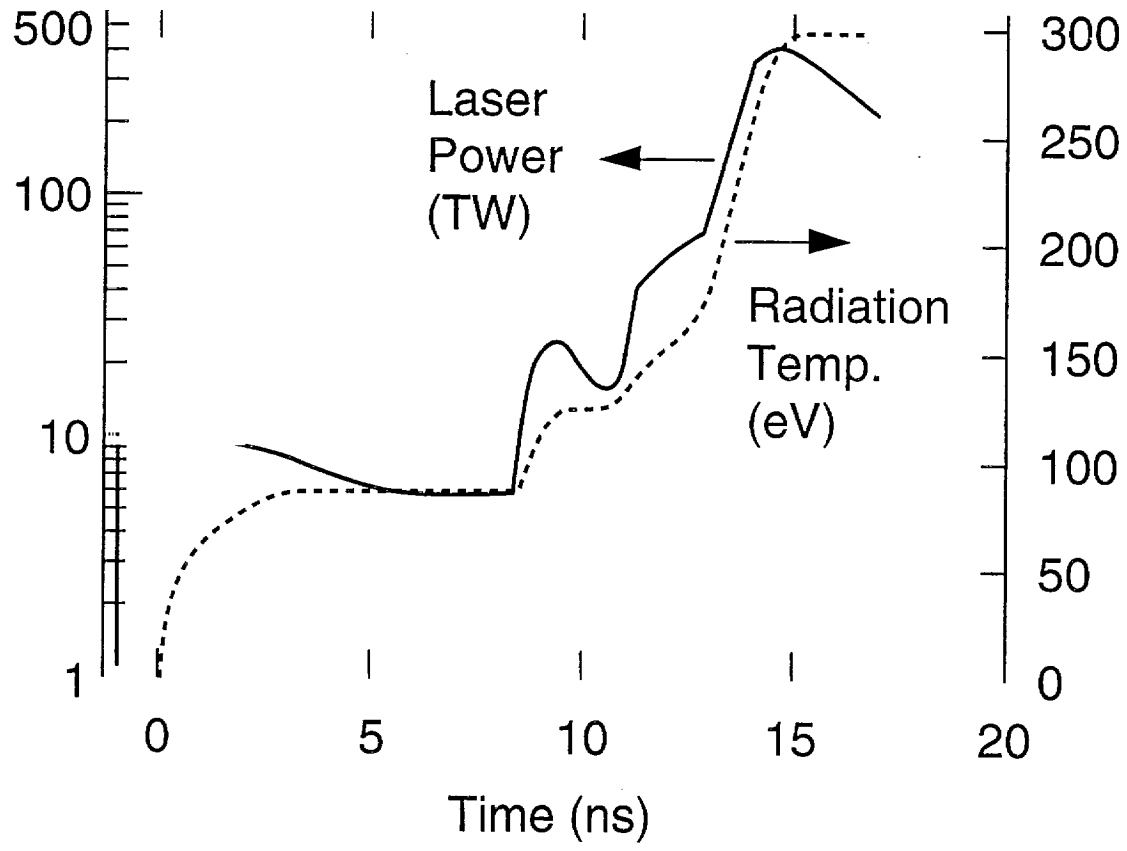
500
100
10
1
300
250
200
150
100
50
0
Laser
Power
(TW)
Radiation
Temp.
(eV)
0
5
10
15
20
Time (ns)

Fig. 3

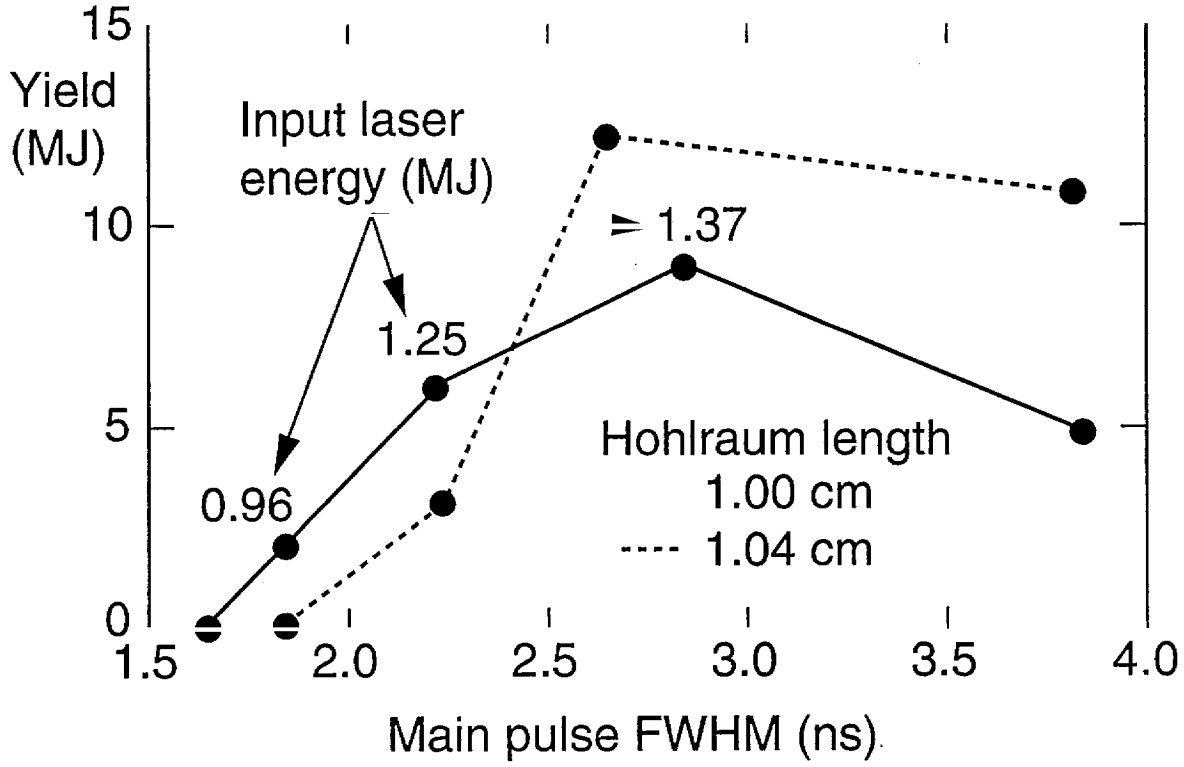
15
Yield
(MJ)
10
5
0
Input laser
energy (MJ)
1.37
1.25
0.96
Hohlraum length
1.00 cm
1.04 cm
1.5
2.0
2.5
3.0
3.5
4.0
Main pulse FWHM (ns)

Fig. 4

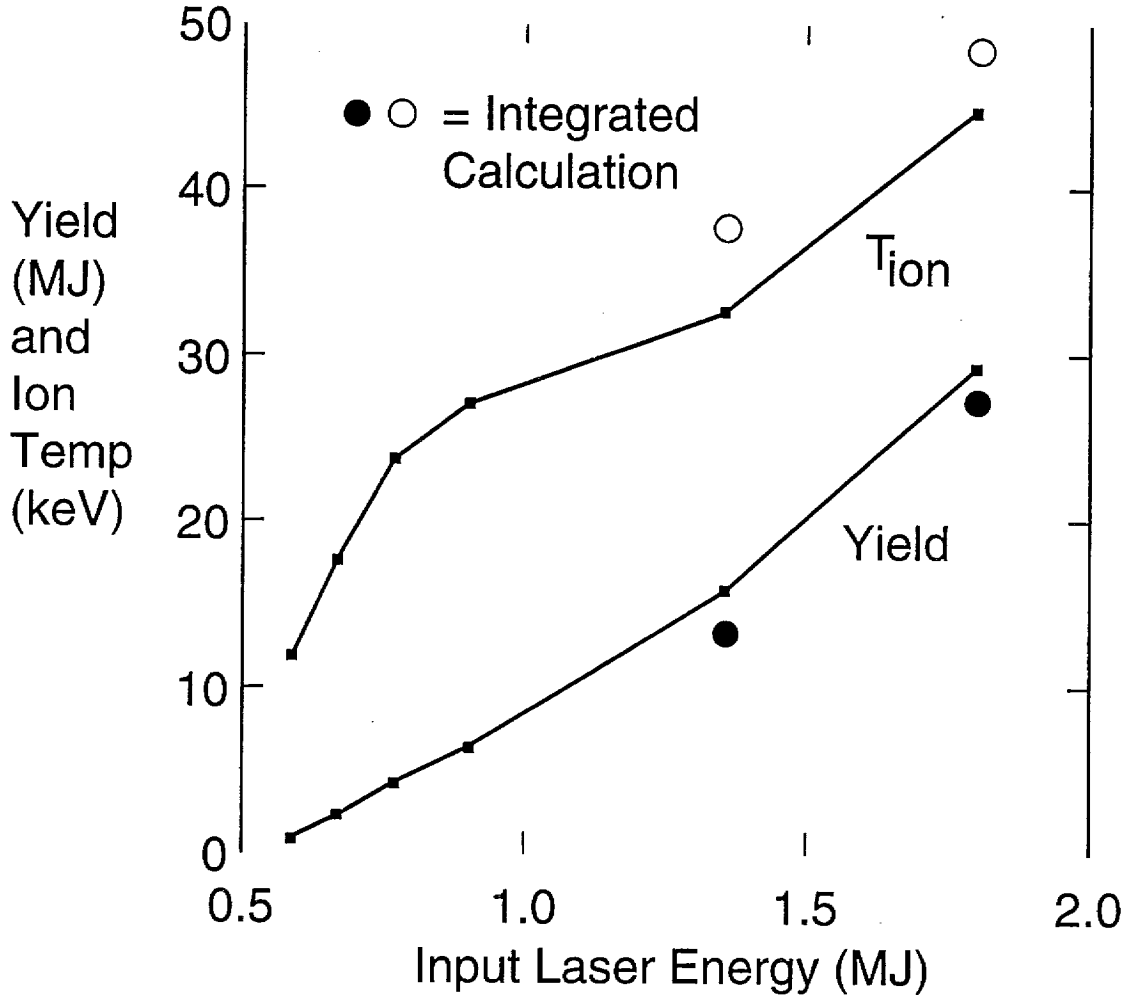
50
40
30
20
10
0
0.5
1.0
1.5
2.0
Yield (MJ) and Ion Temp (keV)
● ○ = Integrated Calculation
T_{ion}
Yield
Input Laser Energy (MJ)

Fig. 5

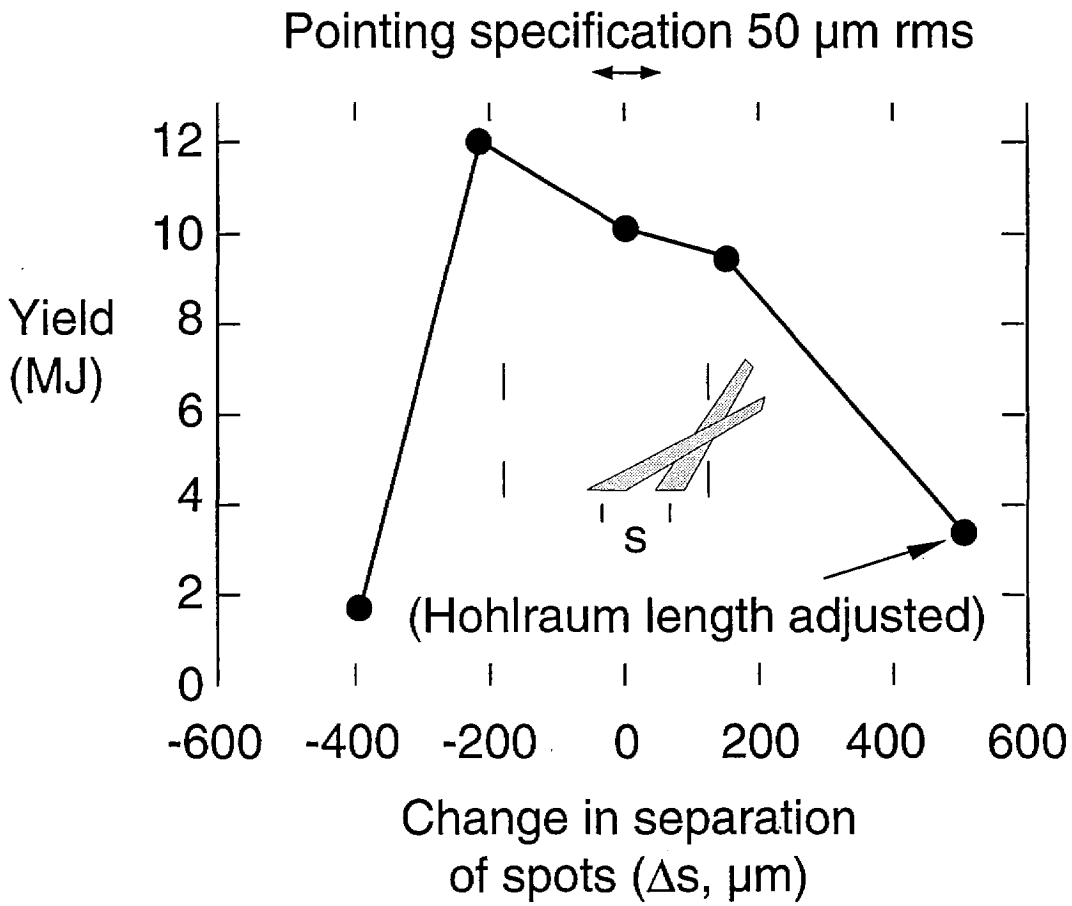
Pointing specification 50 μm rms
Yield
(MJ)
12
10
8
6
4
2
0
s
(Hohlraum length adjusted)
-600
-400
-200
0
200
400
600
Change in separation
of spots (Δs, μm)

Fig. 6